

Text S1. Calibration schemes of EcH₂O-iso and mHM and their coupled N modeling

Model calibrations for both EcH₂O-iso and mHM couplings followed a step-by-step strategy, that is, the discharge simulations were firstly calibrated against the discharge observations at station Silberhütte (the outlet station of the testing catchment); then, parameters of EcH₂O-iso and mHM were fixed and their coupled nitrate-N ($NO_3^- - N$) simulations of HiWaQ-N were calibrated against the daily $NO_3^- - N$ concentration observations.

(1) Discharge calibration of the EcH₂O-iso model. Given the relatively large number of parameters in the EcH₂O-iso model, parameter sensitivity analysis was firstly conducted using the Morris method, similar to the work of Yang et al. (2021) in a headwater catchment Schäferfalta, while here we used the data at the Silberhütte station. We selected 35 most sensitive parameters for the calibration. A Monte Carlo based multi-criteria calibration method was used. In total of 200 000 model runs were firstly conducted based on randomly generated parameter sets (the radial-based Latin-Hypercube sampling strategy). Three discharge performance metrics (i.e., Kling-Gupta Efficiency KGE, the log-transformed KGE and percentage bias PBIAS) were computed for each model run and ranked respectively among all runs (i.e., the empirical cumulative distribution function -CDF for each criterion). A threshold quantile was iteratively determined among the CDFs, above which the common best 500 runs were detected (representing the modelling uncertainty). Because this study was intended to test the initial coupled modelling, we selected one of the best common runs, as presented in **Fig. 5a**. The parameter values and corresponding modelled hydrological fluxes and state variables can be found the associated data repository (see also the “Data availability” statement in the main text).

(3) Discharge calibration of the mHM model. The mHM discharge simulations were generally following the calibrations of the mHM-Nitrate model in Yang et al. (2018) and Yang et al. (2022a) in the whole Selke catchment, while only using the data in the Silberhütte sub-catchment. The Dynamically Dimensioned Search - DDS method (Tolson and Shoemaker, 2007) was used because of its efficiency for computationally demanding models. An aggregated objective function was constructed based on discharge performance metrics Nash-Sutcliffe Efficiency - NSE and the log-transformed NSE (lnNSE), that is,

$$OF = \min\left\{\sqrt[6]{(1 - NSE)^6 + (1 - \ln NSE)^6}\right\} \quad (S1)$$

The parameter values and corresponding modelled hydrological fluxes and state variables can also be found at the open repository. For details of in-depth model calibrations and uncertainty analysis, please refer to (Yang et al., 2018).

(3) Calibration schemes of the coupled HiWaQ-N model. For both of the EcH₂O-iso coupling and the mHM coupling, the DDS method was used for calibrating $NO_3^- - N$ simulations. Performance metrics and objective function for $NO_3^- - N$ were the same as eq.S1. An python script that helps arranging the coupling for multi-run calibrations was also provided, together with the HiWaQ source code (see also the “Code availability” statement in the main text).

Table S1. Major hydrological implementation comparisons between the EcH₂O-iso model and the mHM model.

Process and technical implementations	EcH ₂ O-iso	mHM
Catchment discretization	<ul style="list-style-type: none"> - Grid-based (two levels of spatial resolution: modeling and climate inputs) - Landscape heterogeneity: various soil types and vegetation types allowed in each grid cell, with external areal proportion information 	<ul style="list-style-type: none"> - Grid-based (multiple levels of spatial resolution: geographic inputs, terrestrial modeling, routing modeling and climate inputs) - Landscape heterogeneity: automatically upscaled from the geographic level to the modeling level(s) using the MPR technique
Drainage and stream network	<ul style="list-style-type: none"> - Externally supplied information of topographic drainage network and mean slope - Independent mask of channel network that allows stream routing computed only in real channel-connected grid cells 	<ul style="list-style-type: none"> - Drainage network follows the main drainage lines that are automatically upscaled from fine-resolution DEM input - Stream routing is mandatory for each grid cell at the routing level, of which spatial resolution can be defined independently from that of the terrestrial modeling
Canopy level	<ul style="list-style-type: none"> - Interceptional storage and throughfall - Canopy evaporation and vegetation transpiration driven by energy balance calculations and depending on intercepted water storage and vegetation properties - Module of vegetation dynamics (growth and decay) included - Calculations looped through each vegetation type and aggregated with weights of areal proportions in each grid cell 	<ul style="list-style-type: none"> - Interceptional storage and throughfall - Actual evapotranspiration (ET) firstly considered at canopy level in fulfilling the potential ET demand and depending on intercepted water storage - No vegetation module - Generic calculations in each grid cell without differentiation of various landuse types
Land surface level	<ul style="list-style-type: none"> - Snowpack accumulation and snowmelt driven by energy balance and melting temperature threshold - Temporary surface ponding for infiltration and surface overland flow - Surface infiltration and re-infiltration calculated by the Green-Ampt method - Return flow included - All infiltration- and saturation-excess water is partitioned into overland flow to down-slope cell and surface runoff component (if channel presents) 	<ul style="list-style-type: none"> - Snowpack accumulation and snowmelt calculation based on parameters of threshold temperature and degree day factor - Effective precipitation (throughfall and snowmelt) partitioned to impervious surfaces (e.g., in urban areas) and pervious areas - Impervious storage used for fulfilling ET demand and direct runoff generation - Effective precipitation in pervious areas is all available for vertical infiltration - No upward return flow
Subsurface level – soils	<ul style="list-style-type: none"> - Three soil layers - Soil parameters (soil moisture constants, soil hydraulic properties, etc.) defined as soil-type dependent and varied exponentially along with the soil profile - Soil water downward transport once the upper layer gets saturated - Upward return flow allowed if lower layer gets saturated due to lateral groundwater inflow - Percolation from the third layer to deeper groundwater storage 	<ul style="list-style-type: none"> - Multiple soil layers defined by the users - Soil parameters regionalized via MPR according to soil properties and introduced global parameters - Soil water downward infiltration according to soil moisture states and an exponential factor (as a model parameter) - No upward return flow
Subsurface level – flow generation	<ul style="list-style-type: none"> - Available water storage: the gravitational water storage of the third soil layer (i.e., the difference between soil moisture and the field capacity) - Lateral groundwater flow generation is calculated using a 1-D kinematic wave approach, considering effective hydraulic conductivity and slope gradient 	<ul style="list-style-type: none"> - Available water storage: the conceptual unsaturated storage that receives all infiltration- and saturation-excess water after soil dynamics - Fast-interflow component is activated once the unsaturated storage exceeds a threshold

	<ul style="list-style-type: none"> - If channel presents, runoff seepage to stream is calculated using an exponential decay function, considering effective hydraulic conductivity and a seepage controlling parameter 	<ul style="list-style-type: none"> - and calculated based on a recession coefficient - Slow-interflow component is calculated based on a recession coefficient and a storage-related exponential factor - Percolation from the unsaturated storage to the conceptual saturated storage
Deeper groundwater level	<ul style="list-style-type: none"> - Available water storage: deeper groundwater storage added by Yang et al. (2021) - Lateral deeper baseflow is calculated using a similar kinematic wave approach as groundwater flow, while only involving the hydrologically active part - If channel presents, deeper baseflow seepage to stream is similarly calculated as groundwater runoff component, but with different seepage parameter - No upward water interactions 	<ul style="list-style-type: none"> - Available water storage: the conceptual saturated storage (the passive retention storage is firstly considered in Yang et al. (2018)) - Baseflow component is calculated based on a recession coefficient - No upward water interactions
Lateral connectivity	<ul style="list-style-type: none"> - Terrestrial lateral exchanges are considered as surface overland flow (might activate surface refiltration), groundwater flow (might activate upward return flow), and deeper baseflow - If channel presents, stream routing is calculated using a nonlinear kinematic wave model with a parameter related to Manning's roughness coefficient 	<ul style="list-style-type: none"> - No terrestrial lateral exchange - Catchment lateral hydrological connectivity is only available through stream channels - Terrestrial flow exports are aggregated or disaggregated if routing resolution is specified differently from terrestrial modeling resolution - Stream flow routing is calculated using the Muskingum routing method

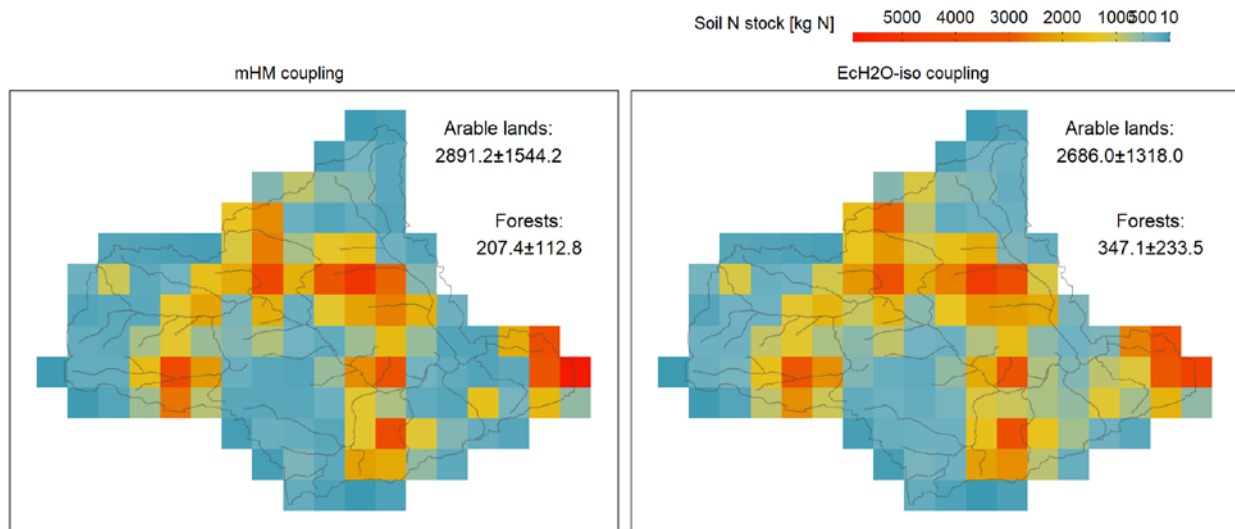


Figure S1. Spatial distributions of simulated average soil N stock based on the mHM coupling and EcH₂O-iso coupling.

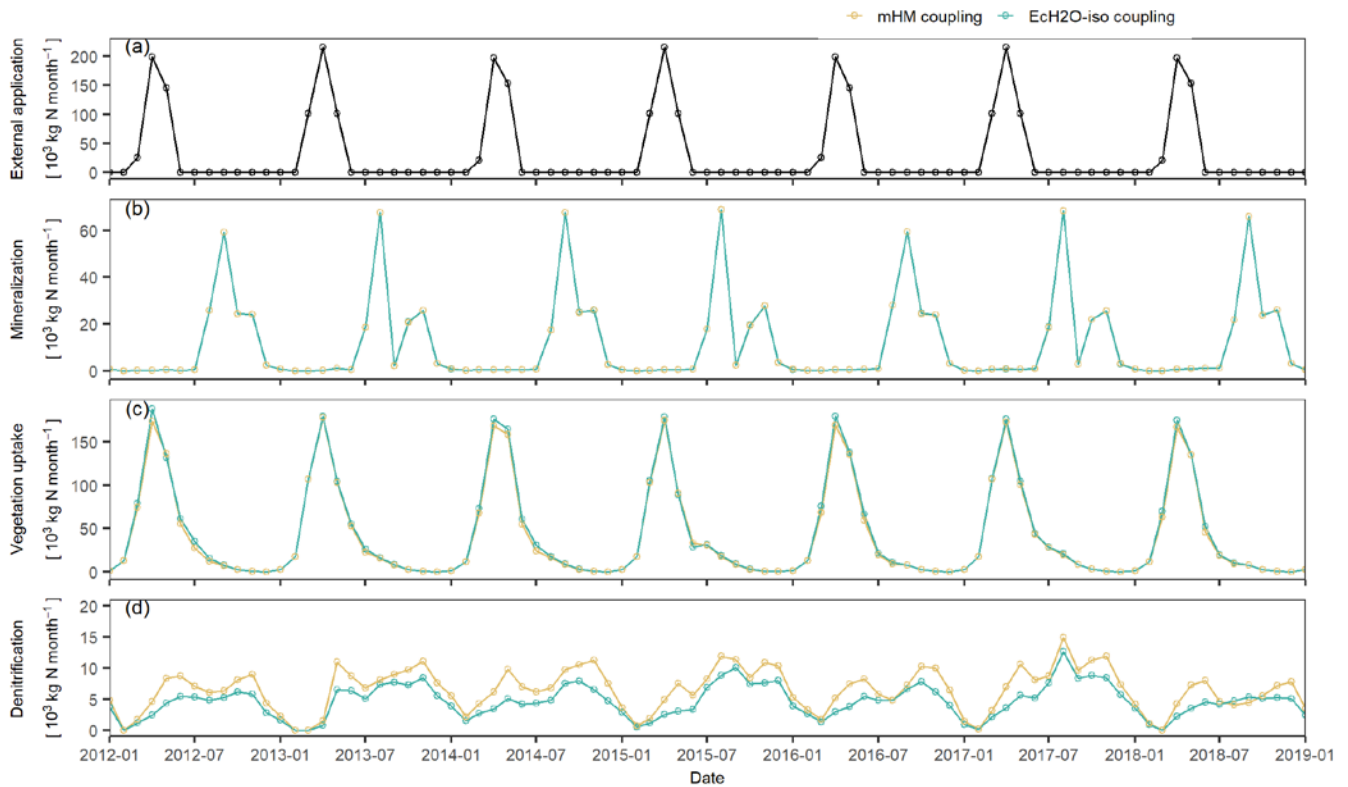


Figure S2. Monthly simulations of catchment-wide N external applications (a, identical for both modelling), mineralization supplies (b), vegetation uptake (c) and denitrification removals (d).

References

- Tolson, B. A. and Shoemaker, C. A.: Dynamically dimensioned search algorithm for computationally efficient watershed model calibration, *Water Resour. Res.*, 43, <https://doi.org/10.1029/2005WR004723>, 2007.
- Yang, X., Jomaa, S., Zink, M., Fleckenstein, J. H., Borchardt, D., and Rode, M.: A new fully distributed model of nitrate transport and removal at catchment scale, *Water Resour. Res.*, 54, 5856–5877, <https://doi.org/10.1029/2017WR022380>, 2018.
- Yang, X., Tetzlaff, D., Soulsby, C., Smith, A., and Borchardt, D.: Catchment Functioning Under Prolonged Drought Stress: Tracer-Aided Ecohydrological Modeling in an Intensively Managed Agricultural Catchment, *Water Resour. Res.*, 57, e2020WR029094, <https://doi.org/10.1029/2020WR029094>, 2021.
- Yang, X., Rode, M., Jomaa, S., Merbach, I., Tetzlaff, D., Soulsby, C., and Borchardt, D.: Functional Multi-Scale Integration of Agricultural Nitrogen-Budgets Into Catchment Water Quality Modeling, *Geophys. Res. Lett.*, 49, e2021GL096833, <https://doi.org/10.1029/2021GL096833>, 2022.